

1 **Genotype-phenotype discrepancy among family members**  
2 **carrying a novel glucokinase mutation: insights into the**  
3 **interplay of GCK-MODY and insulin resistance**

4 Shuhui Ji<sup>1,#</sup>, Hua Shu<sup>1,#</sup>, Hongqiang Zhao<sup>2,3,#</sup>, Yuanyuan Ye<sup>1</sup>, Xuan Liu<sup>1</sup>, Shanshan  
5 Chen<sup>1</sup>, Ying Yang<sup>1</sup>, Wenli Feng<sup>1</sup>, Jingting Qiao<sup>1</sup>, Jinyang Zhen<sup>1</sup>, Xiong Yang<sup>2,3</sup>, Ziyue  
6 Zhang<sup>1</sup>, Yu Fan<sup>1</sup>, Yadi Huang<sup>1</sup>, Qing He<sup>1</sup>, Minxian Wang<sup>2,3,4,5,6,7,‡</sup>, Kunlin Wang<sup>1,‡</sup>,  
7 Ming Liu<sup>1,‡</sup>

8

9 <sup>1</sup> Department of Endocrinology and Metabolism, Tianjin Medical University General  
10 Hospital, Tianjin, 300052, China

11 <sup>2</sup> National Genomics Data Center, China National Center for Bioinformation, Beijing,  
12 China

13 <sup>3</sup> Beijing Institute of Genomics, Chinese Academy of Sciences, Beijing, China

14 <sup>4</sup> College of Future Technology, Sino-Danish College, University of Chinese Academy  
15 of Sciences, Beijing, 100049, China.

16 <sup>5</sup> Department of Cardiovascular Surgery, Zhongnan Hospital of Wuhan University,  
17 Wuhan 430071, China

18 <sup>6</sup> Hubei Provincial Engineering Research Center of Minimally Invasive Cardiovascular

**NOTE: This preprint reports new research that has not been certified by peer review and should not be used to guide clinical practice.**

19 Surgery, Wuhan 430071, China

20 <sup>7</sup>Wuhan Clinical Research Center for Minimally Invasive Treatment of Structural

21 Heart Disease, Wuhan 430071, China

22 #Authors contribute equally to the work.

23 ‡To whom correspondence may be addressed. Ming Liu, Department of

24 Endocrinology and Metabolism, Tianjin Medical University General Hospital, #154

25 Anshan Road, Heping District, Tianjin, 300052, China. Email: [mingliu@tmu.edu.cn](mailto:mingliu@tmu.edu.cn);

26 Kunling Wang, email: [zp-sd@126.com](mailto:zp-sd@126.com); Minxian Wang, email: [wangmx@big.ac.cn](mailto:wangmx@big.ac.cn)

27

28

29

30

31

32

33

34

35

36

## 37 **Abstract**

38 **Aims/Hypothesis:** Heterozygous inactivating mutations in the glucokinase (GCK)  
39 gene are known to cause maturity-onset diabetes of the young (GCK-MODY). We  
40 identified a novel variant of uncertain significance (VUS) GCK mutation (c.77A>T,  
41 p.Q26L) in two family members presenting markedly different severities of diabetic  
42 phenotypes. This study aimed to elucidate the potential diabetogenic effect of GCK-  
43 Q26L and to explore the mono- and poly-genetic background attributing to different  
44 diabetes phenotypes.

45 **Methods:** Whole-exome sequencing (WES) and genetic analyses, including  
46 polygenic risk score (PRS) assessments, were performed in three members of a family  
47 with early-onset diabetes. To elucidate the impact of the GCK-Q26L mutation on  
48 glucose homeostasis, a global knock-in mouse model harboring this mutation in both  
49 heterozygous and homozygous states was generated. Insulin content and insulin  
50 secretion response to glucose and potassium were evaluated in isolated islets.  
51 Furthermore, the effects of dorzagliatin (a glucokinase activator, GKA) and liraglutide  
52 (a glucagon like peptide 1 receptor agonist, GLP-1RA) on glucose tolerance and  
53 insulin secretion were assessed in GCK-Q26L mutant mice.

54 **Results:** The proband, who inherited the GCK-Q26L mutation from her father  
55 (presenting with non-progressive, mildly elevated blood glucose), exhibited severe  
56 diabetic phenotypes including polydipsia, polyuria, polyphagia, weight loss, and

57 ketosis, accompanied by significant dyslipidemia. Genetic analyses revealed that the  
58 proband's severe phenotypes and metabolic profiles were associated with a high  
59 polygenic risk score (PRS) for insulin resistance that was inherited from her mother.  
60 Global heterozygous GCK-Q26L knock-in mice showed a mild increased fasting  
61 blood glucose, impaired glucose tolerance (IGT), and decreased serum insulin.  
62 Homozygous GCK-Q26L mice presented more severe phenotypes compared to their  
63 heterozygous counterparts, confirming the diabetogenic nature of the GCK-Q26L  
64 mutation. Further analyses indicated that GCK-Q26L did not affect insulin sensitivity  
65 and islet insulin content. However, GCK-Q26L blunted islet responsiveness to  
66 different glucose concentrations and markedly impaired glucose-stimulated insulin  
67 secretion (GSIS) without affecting potassium chloride-stimulated insulin secretion  
68 (KSIS) and glucose inhibitory effects on glucagon secretion. Both GKA and GLP-  
69 1RA enhanced insulin secretion and improved glucose tolerance in mutant mice.

70 **Conclusions/Interpretation:** This study demonstrates that GCK-Q26L is a GCK-  
71 MODY causing mutation. The interplay of GCK-Q26L with a high PRS for insulin  
72 resistance contributes to severe diabetic phenotypes. The findings not only expand the  
73 list of GCK-MODY causing mutations originally classified as VUS mutations, but  
74 also provides insights into interactions of GCK-MODY with polygenic risks of type 2  
75 diabetes, highlighting the importance of considering polygenic backgrounds in the  
76 assessment and management of monogenic diabetes.

77 Keywords: monogenic diabetes, glucokinase, GCK-MODY, insulin resistance,  
78 polygenic risk score (PRS)

79

## 80 **Research in Context**

81 What is already known about this subject?

82 Heterozygous inactivating mutations in the GCK gene cause GCK-MODY, an  
83 autosomal dominant disorder characterized by mild hyperglycemia present from birth.

84 Insulin resistance can be influenced by multiple genetic polymorphisms, contributing  
85 to varying diabetes phenotypes.

86 What is the key question?

87 Is the newly discovered GCK mutation pathogenic?

88 Do the interactions between the GCK mutation and PRS for insulin resistance  
89 influence the phenotypic variability in patients carrying GCK-MODY?

90 What are the new findings?

91 The study demonstrates GCK-Q26L impairs GSIS and causes diabetes, establishing it  
92 as a novel GCK-MODY causing mutation originally classified as a VUS mutation.

93 The GCK-Q26L knock-in mouse line replicates phenotypes of GCK-MODY in  
94 humans, establishing it as an excellent model for GCK-MODY.

95 The phenotypic variability in patients with GCK-MODY can be significantly  
96 influenced by high-risk genetic predisposition of type 2 diabetes.

97 Both GKA and GLP-1RA enhance insulin secretion and improve glucose tolerance in  
98 GCK-Q26L mutant mice, suggesting that they are favorite options for treatment of  
99 patients with GCK-MODY and insulin resistance.

100 How might this impact clinical practice in the foreseeable future?

101 Recognizing atypical presentations of monogenic diabetes influenced by polygenic  
102 factors can enhance diagnostic accuracy and personalized management.

103 Genetic testing and polygenic risk score assessments can help identify patients at  
104 higher risk of severe phenotypes, allowing for earlier and more targeted interventions.

105

## 106 **Background**

107 Glucokinase (GCK), a key enzyme in the glycolytic pathway, plays a critical role in  
108 glucose metabolism. It acts as a glucose sensor in pancreatic  $\beta$  cells and regulates  
109 insulin secretion in response to blood glucose levels [1, 2]. The unique kinetic  
110 properties of GCK make it ideal for this regulatory role, as it responds to even small  
111 changes in glucose concentration within the physiological range [2, 3]. Heterozygous  
112 inactivation mutations of GCK are known to cause maturity-onset diabetes of the  
113 young type 2 (MODY 2, also known as GCK-MODY), an autosomal dominant form

114 of diabetes. These GCK inactivation mutations impair enzymatic activity, affecting  
115 glucose sensing of pancreatic  $\beta$  cells, resulting in a higher set point for insulin  
116 secretion, and therefore leading to mild and non-progressive elevated fasting blood  
117 glucose (FBG) from an early age [4, 5]. Notably, unlike other types of diabetes, GCK-  
118 MODY does not typically increase the risks of chronic micro- and macrovascular  
119 complications of diabetes [6]. Therefore, the current recommendations for the  
120 management of GCK-MODY emphasize lifestyle management and regular blood  
121 glucose monitoring rather than active treatment with hypoglycemic agents [6, 7].  
122 However, the clinical presentation of GCK-MODY can vary significantly among  
123 individuals, even within the same family. The underlying mechanisms for this  
124 variability remain incompletely understood.

125 Insulin resistance associated with multiple genetic and environmental factors is a key  
126 feature of type 2 diabetes (T2D) [8]. Recent studies have identified various genetic  
127 polymorphisms contributing to insulin resistance, each adding a small risk but  
128 cumulatively having a significant impact [9]. A high polygenic risk score (PRS) for  
129 insulin resistance aggregates the effect of numerous risk alleles, increasing the  
130 likelihood of T2D development [10, 11]. Additionally, a high PRS for T2D may also  
131 interact with monogenic diabetes causing mutations, leading to atypical and severe  
132 diabetic phenotypes that challenge the traditional approaches for classification and  
133 management of different types of diabetes [8, 12-14]. Understanding the interaction  
134 between these genetic factors is crucial for developing personalized treatment

135 strategies [15].

136 In this study, we identified a novel variant of uncertain significance (VUS) GCK  
137 mutation (c.77A>T, p.Q26L) in two members of a family exhibiting markedly  
138 different severities of diabetic phenotypes. A global knock-in mouse model  
139 established that GCK-Q26L impaired insulin secretion of  $\beta$  cells response to glucose  
140 and caused an increase of FBG and an impairment of glucose tolerance, thereby  
141 confirming this mutation is a GCK-MODY causing mutation. Genetic analyses  
142 revealed the interplay between the GCK-MODY mutation and a high PRS for insulin  
143 resistance contributed to the severe diabetic phenotypes in the proband carrying GCK-  
144 Q26L. The study not only expands the list of GCK-MODY causing mutations  
145 originally classified as VUS mutations, but also highlights genetic bases underlying  
146 phenotype heterogeneities of patients with monogenic diabetes.

147

## 148 **Materials and Methods**

149 **Patients.** The clinical information of the proband and her family members was  
150 detailed in Table 1, collected and documented in Tianjin Medical University General  
151 Hospital. Informed consent was obtained from all family members. The study was  
152 approved by the Tianjin Medical University General Hospital Ethics Committee  
153 (IRB2017-047-01).

154 **Genetic Testing and Analyses.** DNA was extracted from proband's white blood cells



155 for targeted gene capture, followed by whole-exome sequencing (WES) utilizing  
156 massive parallel next-generation sequencing (NGS). The identified GCK gene  
157 mutation was further confirmed by Sanger sequencing, the primers for the forward-  
158 and reverse-strand were 5'-TGTGGGGGAGATGCCCCG-3' and 5'-  
159 ACCAGAGGAGCCAAGGGTGAG-3', respectively. Members of the proband's  
160 family (father, mother and grandfather) were recruited and checked for the mutation  
161 using Sanger sequencing. Furthermore, the family members (father and mother) also  
162 underwent WES sequencing.

163 **Definitions for Insulin Resistance.** Insulin resistance (IR) was measured as the ratio  
164 of triglycerides (TG) to high-density lipoprotein cholesterol (HDL-C) as described  
165 elsewhere [9, 16-19] (ESM Fig. 4). To correct the potential effect of cholesterol  
166 lowering medications, we adjusted the levels of TG and HDL-C before calculating IR  
167 with detailed adjustment in ESM Table 4.

168 **Genotype quality control and imputation.** The proband trios were genotyped by  
169 Affymetrix Axiom whole-genome Asian Screening Array (ASA Array) with calling  
170 rate > 99%. Kingship (ESM Table1) and sex (ESM Table2) were further validated  
171 with genetically inferred ones. The data was merged with non-close related samples  
172 from the 1000 Genomes Project with ambiguous variants (A/T or G/C alleles)  
173 removed. This was followed by a series of quality controls in samples with a  
174 missingness rate > 5%, or heterozygosity out of 5 standard deviations were excluded,

175 and variants with a missing rate > 1% or Hardy-Weinberg equilibrium with a P-value  
176  $< 1 \times 10^{-6}$  were excluded. Then, principal component analysis (PCA) was  
177 conducted, and ancestry was inferred by the PCA clusters. Finally, the genotype was  
178 further imputed on the TOPMed imputation server [20] (ESM Fig. 3), and variants  
179 with imputation quality score (INFO) < 0.8 were removed in subsequent analysis.

180 **PRS assessment.** We directly utilized the polygenic scores model for insulin  
181 resistance developed by Lotta et al.[8] from the PGS Catalog and calculated the PRS  
182 for our datasets together with 1000 Genomes Project East Asian samples by PLINK  
183 2.0 [21]. To confirm the association between PRS and IR, we also calculated the PRS  
184 for the samples (424,068 passed quality control) from the UK Biobank (ESM Table 3)  
185 under application number 89885, following the same procedures. The PRS was  
186 further corrected by the value of principal components (PCs) for potential population  
187 structure and batch effects and standardized to normal distribution for further  
188 statistical analysis.

189 **Mice.** We commissioned GemPharmatech Co., Ltd. to create a global knock-in GCK-  
190 Q26L mouse model. The Q26L site-directed mutagenesis was introduced in exon 2 of  
191 mouse GCK-201, changing the codon for the 26th amino acid from CAG to CTG and  
192 inserting MYC before the stop codon (ESM. Fig.1a). All mice were bred on a  
193 C57BL/6J background and housed in temperature (22–25 °C) and humidity (55 ± 5%)  
194 controlled rooms with a 12-hour light/dark cycle. All animal experimental protocols

195 were approved by the Internal Animal Welfare Committee at Chu Hsien-I Memorial  
196 Hospital (Metabolic Diseases Hospital) of Tianjin Medical University.

197 **Glucose and insulin tolerance.** Mice were fasted for 6 hours before intraperitoneal  
198 glucose tolerance tests (IPGTT). Glucose was administered via intraperitoneal  
199 injection at 2 g/kg body weight. Blood glucose was measured from the tail vein at 0,  
200 15, 30, 60, and 120 minutes using an automated glucose meter (Roche, ACCU-CHEK,  
201 Germany). ELISA kits were used to measure plasma insulin (EZassay, China), and  
202 glucagon (Ruixin, China). For the intraperitoneal insulin tolerance test (IPITT), after a  
203 4-hour fast, mice received an intraperitoneal injection of 0.7 U/kg body weight of  
204 insulin (Aspart, Novo Nordisk A/S, Denmark). Dorzagliatin (Desano, China) and  
205 Liraglutide (Solarbio, China) were administered to mice by gavage or intraperitoneal  
206 injection, respectively, 90 minutes before the start of the IPGTT.

207 **Measurement of insulin and glucagon secretion.** Islet isolation, glucose-stimulated  
208 insulin secretion (GSIS), and potassium-stimulated insulin secretion (KSIS) were  
209 performed as previously described [22], glucose-inhibited glucagon secretion was  
210 performed simultaneously with GSIS. For the dose-dependent effects of glucose on  
211 insulin secretion, isolated pancreatic islets were sequentially cultured in Krebs-Ringer  
212 bicarbonate HEPES (KRBH) buffer with glucose concentrations of 2.8 mM, 3.3 mM,  
213 4.5 mM, 5.6 mM, and 7 mM for 2 hours each. After incubation, supernatants were  
214 collected, and the islets were homogenized. Secreted insulin and islet insulin content

215 were measured using ELISA kits (EZassay, China). The secretion efficiency was  
216 calculated with secreted insulin in the media normalized to islet insulin content.

217 **Islet perfusion assays.** Islet perfusion assays were performed as previously described  
218 [22]. The liquid input flow rate was 150  $\mu$ l/min, with samples collected every minute.  
219 Insulin secretion at each time point was quantified using the Wide Range Insulin  
220 Assay Kit (EZassay, China) according to the manufacturer's instructions.

221 **Western blot analysis.** Equal amounts of islet proteins were loaded onto 4-12%  
222 NuPage gradient gels (Thermo, USA), while other tissues were loaded onto 12.5%  
223 gels (US EVERBRIGHT, China). The antibodies used in this study were as follows:  
224 anti-GCK (Cat: A00884-1, BOSTER, China), anti-c-MYC (Cat: RMYC-45A-2, ICL,  
225 USA), anti-GAPDH (Cat: AC033, Abclonal, China), anti-insulin (homemade).

226 **Immunofluorescence.** Mouse pancreas was fixed, sectioned, and stained with  
227 different primary antibodies followed by Alexa-Fluor-conjugated secondary  
228 antibodies. The antibodies used in this study were as follows: anti-insulin  
229 (homemade), anti-glucagon (Cat: G2654, Sigma, USA), anti-somatostatin (Cat:  
230 ab30788, abcam, USA). Fluorescent images were visualized using an Axio Imager  
231 M2 microscope (Carl Zeiss, Germany).

232 **Statistics.** All experiments were performed independently at least three times. Data  
233 are presented as means  $\pm$  SEM. Statistical analyses were conducted using GraphPad  
234 Prism 8 software. An unpaired Student's t-test was used for data analysis, with a

235 threshold of  $P < 0.05$  to declare statistical significance.

236

## 237 **Results**

### 238 **Identification of a novel variant of uncertain significance (VUS) GCK mutation**

239 **in a family with early onset diabetes.** In the clinic, we observed a special case of  
240 diabetes. The female proband was diagnosed with diabetes at age teens, presenting  
241 with polydipsia, polyuria, polyphagia, weight loss, and ketosis. Her body mass index  
242 (BMI) was 22.66 kg/m<sup>2</sup>, and islet autoantibodies were all negative. Initial FBG was  
243 6–7 mmol/L, 2hBG was 15–18 mmol/L, and HbA1c was 113.12 mmol/mol (12.5%).  
244 The result of the 75g oral glucose tolerance test (OGTT) confirmed the diagnosis of  
245 diabetes and indicated the presence of insulin resistance and inadequate insulin  
246 secretion in response to glucose load. (Fig. 1a). She was treated with Metformin (0.5 g  
247 TID) and Insulin glargine (18 U QN), with occasional monitoring showing FBG of 5–  
248 7 mmol/L and 2hBG of 13–14 mmol/L. She continued this treatment inconsistently,  
249 without dietary control, regular exercise, or routine SMBG. After 2.5 years, she  
250 discontinued insulin and continued Metformin (0.5 g TID), with occasional FBG  
251 readings of 6–7 mmol/L. Five years post-diagnosis, her FBG increased to 7.5–13.2  
252 mmol/L, HbA1c to 132.79 mmol/mol (14.3%), and BMI to 26.76 kg/m<sup>2</sup>. Her regimen  
253 was changed to Metformin (0.5 g TID), Insulin aspart (8-6-6 U before meals), and  
254 Insulin glargine (12–16 U QN), but glycemic control remained poor, with FBG of 7–

255 10 mmol/L. Her father was diagnosed with diabetes at thirties, treated with Metformin  
256 0.5 g BID and Vildagliptin 50 mg BID, with FBG of 5–7 mmol/L. Seven years later,  
257 his regimen was changed to Metformin 0.5 g TID and occasional Dapagliflozin,  
258 maintaining FBG at 6.5 mmol/L and HbA1c at 60.66 mmol/mol (7.7%). Her  
259 grandfather was diagnosed with diabetes at fifties, managed with oral hypoglycemic  
260 agents. Her mother was found to have pre-diabetes at forties based on blood glucose  
261 and HbA1c levels. Clinical details of the proband and her family were summarized in  
262 Table 1.

263 Given the proband's negative islet autoantibodies and family history, we suspected  
264 monogenic diabetes and performed genetic screening. DNA sequencing revealed a  
265 novel heterozygous missense mutation, c.77A>T, in exon 2 of the GCK gene,  
266 resulting in a glutamine-to-leucine substitution at position 26 (p.Q26L), which had not  
267 been reported yet. According to American College of Medical Genetics and Genomics  
268 (ACMG) and the Association for Molecular Pathology (AMP) in 2015 guidelines, the  
269 mutation was classified as a variant of uncertain significance (VUS) with evidence  
270 PM1+PM2+PP2. Pedigree analysis showed that the proband's father had the same  
271 heterozygous mutation, while the grandfather and mother did not (Fig. 1b, c).

272 Based on these findings, the proband's diabetes type and the role of the GCK-Q26L  
273 mutation in her complex diabetic phenotype remain unclear. However, the father's  
274 glycemic profile aligned with typical GCK-MODY characteristics. Therefore, further

275 experiments were conducted to assess the impact of the GCK mutation on protein  
276 function.

277

278 **GCK-Q26L is a GCK-MODY causing mutation.** Since GCK-Q26L was classified  
279 as a VUS and the proband presented atypical clinical features of GCK-MODY, it  
280 remained to be determined whether GCK-Q26L is a diabetes causing mutation. We  
281 therefore established a global knock-in mouse model expressing MYC-tagged GCK-  
282 Q26L (ESM Fig. 1a). Western blot confirmed the specific expression of MYC-tagged  
283 mutant GCK in the liver and islets in a dose-dependent manner in GCK-Q26L  
284 heterozygous (Het) and homozygous (Hom) mice (ESM Fig. 1b). We had monitored  
285 body weight (BW) and FBG of mutant and wild-type (WT) male mice for 16 weeks.  
286 Although the GCK-Q26L mutation did not affect BW, it caused mild, non-progressive  
287 elevation of FBG in Het mice, with further elevation observed in Hom mice (Fig. 2a,  
288 b). To investigate whether abnormal circulating levels of insulin or glucagon were  
289 associated with elevated FBG, we examined fasting serum insulin and glucagon levels.  
290 Our findings showed that although glucagon levels were unaffected, serum insulin  
291 levels were decreased in 16-week-old mutant mice (Fig. 2c, d). We therefore  
292 performed intraperitoneal glucose tolerance test (IPGTT) and found that Het and Hom  
293 mice exhibited significantly impaired glucose tolerance and lower serum insulin  
294 levels compared to that of WT mice at 3 weeks of age (Fig. 2e, f). The severities of

295 decreased serum insulin and impaired glucose tolerance did not further worsen in 16-  
296 week-old mutant mice (Fig. 2g, h). The phenotype of female mice was similar to that  
297 of male mice but less severe (ESM Fig. 2). These data established that GCK-Q26L  
298 caused non-progressive mild hyperglycemia representing one of classic clinical  
299 features of GCK-MODY, confirming that GCK-Q26L is a GCK-MODY mutation.

300

301 **GCK-Q26L does not affect insulin sensitivity and islet insulin content.** Since GCK  
302 is also expressed in hepatocytes, we asked whether GCK-Q26L affected insulin  
303 sensitivity. We performed intraperitoneal insulin tolerance test (IPITT) and found that  
304 GCK mutant did not affect insulin sensitivity (Fig. 3a, b), suggesting that  
305 hyperglycemia was mainly due to decreased circulating insulin. To investigate  
306 whether reduced serum insulin in Het and Hom male mice is caused by decreased to  
307 islet insulin content or insulin secretion, we measured insulin content by two  
308 independent approaches (western blots and insulin enzyme-linked immunosorbent  
309 assays, ELISA). Both methods consistently showed no substantial differences in  
310 insulin content in islets of Het and Hom mice compared to WT mice (Fig. 3c-f). The  
311 ratio of proinsulin-to-insulin was also not affected (Fig. 3f). Immunofluorescence  
312 analysis revealed no impact of the mutation on the abundance and intraislet  
313 composition of insulin-positive, glucagon-positive, and somatostatin-positive cells  
314 among three groups (Fig. 3h). Furthermore, western blot results showed no significant



315 differences in endogenous GCK protein expression in the islets among the three  
316 groups, indicating that the GCK-Q26L did not affect protein levels of endogenous  
317 GCK (Fig. 3d, g).

318

319 **GCK-Q26L impairs glucose-stimulated insulin secretion without affecting**  
320 **potassium-stimulated insulin secretion and glucose-inhibited glucagon secretion.**

321 Since the GCK-Q26L caused a decrease of circulating insulin without affecting islet  
322 insulin content (Fig. 2-3), we next asked whether it impair insulin secretion. Insulin  
323 secretion was monitored in isolated islets exposed to different glucose concentrations  
324 (2.8 mM, 3.3 mM, 4.5 mM, 5.6 mM, 7 mM). We found that the curve of glucose  
325 concentration-dependent insulin secretion was shifted to right in Het mice (Fig. 4a),  
326 suggesting that the glucose threshold for insulin secretion was increased in GCK-  
327 Q26L mice. In addition, insulin secretion response to even higher glucose (16.7 mM)  
328 was also impaired in Het islets and the response was further diminished in Hom islets  
329 (Fig. 4b). Islet perfusion tests with different glucose concentrations further supported  
330 these observations (Fig. 4c). However, despite defects in response to glucose, GCK-  
331 Q26L did not affect insulin secretion response to potassium in both tests of potassium  
332 chloride-stimulated insulin secretion (KSIS) and islet perfusion (Fig. 4d, e).  
333 Furthermore, no differences were observed in glucose-inhibited glucagon secretion  
334 (GIGS) in Het and Hom mutant mice (Fig. 4f). These data demonstrated that GCK-

335 Q26L impaired the function of GCK as a glucose sensor in  $\beta$  cells, impeding GSIS  
336 without affecting KSIS and GIGS.

337

338 **Dorzagliatin restores the glucose threshold for insulin secretion and ameliorates**  
339 **glucose tolerance in GCK-Q26L mice.** Dorzagliatin, a novel allosteric glucokinase  
340 activator (GKA), improved glycaemic control and was approved in China for the  
341 treatment of adult patients with type 2 diabetes [23, 24]. To evaluate the effects of  
342 dorzagliatin on insulin secretion and glucose tolerance in GCK-Q26L mice, we firstly  
343 treated mice with oral administrations of dorzagliatin, measured fasting blood glucose  
344 and insulin levels 90 minutes after treatment, and then performed IPGTT. We found  
345 that dorzagliatin significantly decreased FBG and increased fasting insulin levels in  
346 both WT, Het, and Hom mutant mice (Fig. 5a, b). IPGTT results further confirmed  
347 improvement of glucose tolerance in mutant mice treated with dorzagliatin (Fig. 5c).  
348 We further analyzed insulin secretion response glucose and found that dorzagliatin  
349 restored the glucose threshold for insulin secretion (Fig. 5d) and improved GSIS (Fig.  
350 5e) in GCK-Q26L mutant islets.

351

352 **Liraglutide amplifies insulin secretion response to glucose and ameliorates**  
353 **glucose tolerance in GCK-Q26L mice.** Since liraglutide, a glucagon-like peptide-1  
354 receptor agonist (GLP-1RA), has an effect of glucose-dependent stimulated insulin

355 secretion, we next asked whether liraglutide could show beneficial effects on insulin  
356 secretion and glucose tolerance in GCK-Q26L mice. We conducted similar  
357 experiments as dorzagliatin treatment shown in Fig. 5. We found that unlike  
358 dorzagliatin, liraglutide did not significantly stimulate insulin secretion in the fasting  
359 state both in WT and mutant mice, and only moderately decreased FBG in GCK  
360 mutant mice compared with dorzagliatin (Fig. 6a, b). However, liraglutide indeed  
361 markedly stimulated insulin secretion and decreased blood glucose 15 minutes after  
362 glucose load (Fig. 6c, d), ameliorating overall glucose tolerance (Fig. 6e). In vitro  
363 experiments using isolated islets further confirmed that liraglutide improved GSIS  
364 (Fig. 6f) and amplified insulin secretion in 5.6 mmol/L glucose (Fig. 6g) in islets  
365 from GCK-Q26L mice. Altogether, these results suggest that while both dorzagliatin  
366 and liraglutide improve glucose homeostasis, they do so through distinct mechanisms.  
367 Dorzagliatin directly enhances the glucose-sensing capability of glucokinase, whereas  
368 liraglutide amplifies insulin secretion in response to glucose.

369

370 **A high PRS for insulin resistance is associated with atypical and more severe**  
371 **diabetic phenotypes in proband.** The experimental evidence above demonstrates  
372 that GCK-Q26L is a GCK-MODY causing mutation. However, although the proband  
373 inherited the mutation from her father who presented typical clinical features of GCK-  
374 MODY, the proband presented more severe hyperglycemia that did not resemble a

375 classic GCK-MODY (Fig. 1 and Table 1), suggesting that additional factors may  
376 contribute to phenotypes of the proband. Indeed, as the disease progressed , the  
377 proband became overweight (BMI 26.76 kg/m<sup>2</sup>) and developed dyslipidemia with a  
378 high Triglyceride (TG) to HDL-cholesterol (HDL-c) ratio, conditions often associated  
379 with insulin resistance [19]. Utilizing data from 424,068 individuals in the UK  
380 Biobank (UKB), we examined the association between the TG/HDL-c ratio, a  
381 surrogate measure of insulin resistance [9, 16-19], with insulin resistance polygenic  
382 scores. Results indicated the PRS was significantly associated with the observed  
383 TG/HDL-c ratio, that higher PRS levels corresponded with increases in the TG/HDL-  
384 c ratio, supporting the relevance of PRS in assessing insulin resistance genetic risk in  
385 the population (Fig. 7a). To explore the genetic predisposition of insulin resistance in  
386 this family, we conducted a PRS analysis and used the East Asian samples from the  
387 1000 Genomes Project samples for evaluate the PRS risk and adjusted for potential  
388 population structure confounding through principal component analysis (PCA) (ESM  
389 Fig. 5a, b). The PRS analysis of the family indicated the proband inherited a high  
390 insulin resistance genetic risk from her mother, who has an IR PRS score ranked in  
391 the top 2% in the study population (Fig. 7b). According to previous studies,  
392 monogenic risk and polygenic scores may jointly influence the risk of disease [14].  
393 These data suggest that the probands' atypical and severe diabetic phenotypes were  
394 associated with high PRS for insulin resistance in addition to GCK mutation.

395

## 396 **Discussion**

397 The identification of the novel GCK-Q26L mutation, originally classified as VUS, in  
398 two members of a family with marked differences in PRS for insulin resistance and  
399 different severities of diabetes adds to the growing complexities of genetic  
400 contributions to the development and progression of diabetes. With multiple  
401 independent approaches, we demonstrated that GCK-Q26L did not affect insulin  
402 biosynthesis and islet insulin content, but impeded glucose sensing of pancreatic  $\beta$   
403 cells, increasing the threshold of glucose concentration for insulin secretion, impairing  
404 GSIS, and therefore causing mild elevated FBG and glucose intolerance. These data  
405 established that GCK-Q26L is indeed a pathogenic mutation causing GCK-MODY.

406

407 GCK-MODY typically presents with mild hyperglycemia that is often managed  
408 without pharmacological intervention due to low risks of diabetes related chronic  
409 complications and the limited efficacy of traditional glucose-lowering medications [4,  
410 6]. However, the presence of insulin resistance can complicate the clinical picture,  
411 leading to more severe hyperglycemia and necessitating therapeutic intervention. The  
412 results from our GCK-Q26L mouse model highlight the potential therapeutic benefits  
413 of using GKA and GLP-1RAs in managing diabetes phenotypes influenced by both  
414 GCK mutations and polygenic risk factors for insulin resistance. Dorzagliatin is a new  
415 a dual-acting GKA that enhances glucokinase activity by binding to its allosteric site,

416 increasing glucose phosphorylation and insulin secretion, thereby improving glycemic  
417 control [23, 25]. In a clinical trial, dorzagliatin directly increases insulin secretion and  
418 glucose sensitivity in patients with GCK-MODY, suggesting that it may be able to  
419 preserve GCK activity in GCK-MODY [26]. Our data further demonstrated that  
420 dorzagliatin restored glucose threshold for insulin secretion and improved GSIS and  
421 glucose intolerance in GCK-Q26L mutant mice (Fig, 5d-e). It is worthy to note that  
422 dorzagliatin can increase insulin secretion in GCK-Q26L mice and decrease blood  
423 glucose even in the fasting state with relatively low FBG in both WT and mutant mice  
424 (Fig. 5a-c). However, there is no increased risk of hypoglycemia in a phase 3 clinical  
425 trial dorzagliatin [23]. It remains to be determined whether this was caused by extra  
426 high dose of dorzagliatin (about 15 times higher dose using in mice in this study than  
427 recommend dose for patients with type 2 diabetes) or due to different responses of  
428 different species.

429

430 In addition to dorzagliatin that directly targets to GCK, GLP-1RAs may also be  
431 considered for the management of patients with GCK-MODY due to its beneficial  
432 effect on glucose-dependent insulin secretion. Indeed, our data demonstrated that  
433 liraglutide enhanced glucose sensing of mutant islets at physiological glucose  
434 concentrations and improved GSIS (Fig. 6). Furthermore, one signal administration of  
435 liraglutide could significantly decrease FBG of mutant mice without affecting FBG of

436 WT mice and markedly improve glucose tolerance (Fig, 6). These beneficial effects  
437 on glucose sensing and insulin secretion along with its role in regulating weight loss  
438 and insulin resistance make liraglutide (and may be other GLP1-RAs) an attractive  
439 option for the management of GCK-MODY, especially in patients with GCK-MODY  
440 with insulin resistance.

441

442 To date, monogenic mutation involved in more than 70 genes have been identified to  
443 cause monogenic diabetes. Some of the biggest challenges for early recognition and  
444 diagnosis of monogenic diabetes are highly variable for disease penetrance and  
445 clinical presentations in patients carrying different mutations in one gene or even the  
446 same mutation in the same gene. Accumulating evidence indicates that genetic and/or  
447 environmental factors may exacerbate or lessen the conditions, and many VUS can  
448 have significant pathogenic effects when combined with other genetic predispositions  
449 [4, 27]. In the current study, we found that the proband who carried a GCK-MODY  
450 causing mutation inherited from her father, also possessed a high PRS for insulin  
451 resistance that may have been inherited in part from her mother, whose PRS for  
452 insulin resistance was in top 1.09<sup>th</sup> percentile (Fig. 7). The elevated PRS may  
453 contribute to proband's atypical presentation including more severe hyperglycemia  
454 and dyslipidemia, supporting an additive effect that monogenic and polygenic factors  
455 may interact. These findings align with recent research indicating that PRS can

456 substantially influence the clinical presentation of monogenic diseases, including  
457 diabetes [28, 29]. This dual influence underscores the complexity of diabetes  
458 pathogenesis and challenges the traditional dichotomy between monogenic and  
459 polygenic diabetes, highlighting the importance of considering polygenic factors even  
460 in cases initially attributed to single-gene mutations [30, 31]. Incorporating  
461 comprehensive genetic assessments, including PRS, into routine diabetes care could  
462 revolutionize how we predict, diagnose, and manage diabetes. Recognizing the role of  
463 PRS might help identify individuals at high risk for severe forms of diabetes,  
464 facilitating earlier interventions and more personalized management strategies [32].  
465 Additionally, understanding the interplay between different genetic factors could lead  
466 to the development of targeted therapies that address specific mechanistic pathways  
467 involved in the disease [33, 34]. Recent studies have demonstrated the potential of  
468 such personalized approaches in improving disease prognosis [35].

469

470 Despite these promising findings, several limitations need to be acknowledged. First,  
471 the study's reliance on a mouse model may not fully capture the complexity of human  
472 GCK-MODY and its interaction with insulin resistance. While the GCK-Q26L mutant  
473 mouse model provides valuable insights, human clinical trials are essential to validate  
474 the efficacy and safety of GKA and GLP-1RAs in GCK-MODY individuals with or  
475 without insulin resistance. Second, the study did not explore the long-term effects of



476 these treatments on beta-cell function and overall metabolic health. Longitudinal  
477 studies are necessary to understand the potential benefits and risks associated with  
478 chronic use of these therapies. Third, the sample size and genetic diversity of the  
479 study population were limited. Future research should include larger, more diverse  
480 cohorts to ensure the generalizability of the findings. Furthermore, exploring gene-  
481 environment interactions will be crucial in elucidating the full impact of monogenic  
482 and polygenic factors on the development and progression of monogenic diabetes.

483

#### 484 **Author contributions**

485 SJ, HS, and HZ designed and conducted experiments and analyzed data; SJ, HS, HZ  
486 YY, XL, SC, WF, JQ, JZ, and ZZ conducted experiments; All other authors revised  
487 the manuscript critically for important intellectual content. MW discussed project and  
488 edited manuscript; ML initiated and oversaw the project, designed the experiments,  
489 and wrote the manuscript.

#### 490 **Acknowledgments**

491 The work was supported by the National Key R&D Program (2022YFE0131400 and  
492 2019YFA0802502), and also by the National Natural Science Foundation of China  
493 (82220108014). We acknowledge the support of Tianjin Municipal Health  
494 Commission (TJWJ2021ZD001), Tianjin Medical University General Hospital  
495 Clinical Research Program (22ZYYLCZD02), Tianjin Municipal Science and

496 Technology Commission (23JCQNJC00680 and 23JCQNJC00670), National Natural  
497 Science Foundation of China (82200892, 82301951, and 81800733), Tianjin  
498 Municipal Education Commission (2021KJ209), Tianjin Medical University  
499 Endocrine and Metabolic Disease the Youth Talent Incubator Program  
500 (2024XKNFM13), Tianjin Key Medical Discipline (Specialty) Construction Project  
501 (TJYXZDXK-030A), and Tianjin Medical University Clinical Special Disease  
502 Research Center - Neuroendocrine Tumor Clinical Special Disease Research Center.

503 **Data availability**

504 Due to local privacy laws and privileged human information, all requests for raw  
505 genotyping and clinical data are subject to prior approval from the local IRB. Analysis  
506 of the UK Biobank data was performed using application 89885. The UK Biobank  
507 data are available to researchers with research inquiries following IRB and UK  
508 Biobank approval ([https://www.ukbiobank.ac.uk/enableyour-research/apply-for-](https://www.ukbiobank.ac.uk/enableyour-research/apply-for-access)  
509 [access](https://www.ukbiobank.ac.uk/enableyour-research/apply-for-access)).The polygenic scores described in this publication are available for download  
510 from the Polygenic Score Catalog ([https:// www.pgscatalog.org](https://www.pgscatalog.org)) under the publication  
511 ID PGP000223

512 **Code availability**

513 The manuscript described a pragmatic approach of publicly available software.  
514 Additional code is available upon request from the authors.

## 515 **References**

- 516 [1] Matschinsky FM (1990) Glucokinase as glucose sensor and metabolic signal generator in  
517 pancreatic beta-cells and hepatocytes. *Diabetes* 39(6): 647-652. 10.2337/diab.39.6.647
- 518 [2] Grimsby J, Sarabu R, Corbett WL, et al. (2003) Allosteric activators of glucokinase: potential  
519 role in diabetes therapy. *Science* 301(5631): 370-373. 10.1126/science.1084073
- 520 [3] Matschinsky FM (2002) Regulation of pancreatic beta-cell glucokinase: from basics to  
521 therapeutics. *Diabetes* 51 Suppl 3: S394-404. 10.2337/diabetes.51.2007.s394
- 522 [4] Stride A, Vaxillaire M, Tuomi T, et al. (2002) The genetic abnormality in the beta cell  
523 determines the response to an oral glucose load. *Diabetologia* 45(3): 427-435. 10.1007/s00125-  
524 001-0770-9
- 525 [5] Osbak KK, Colclough K, Saint-Martin C, et al. (2009) Update on mutations in glucokinase  
526 (GCK), which cause maturity-onset diabetes of the young, permanent neonatal diabetes, and  
527 hyperinsulinemic hypoglycemia. *Hum Mutat* 30(11): 1512-1526. 10.1002/humu.21110
- 528 [6] Steele AM, Shields BM, Wensley KJ, Colclough K, Ellard S, Hattersley AT (2014) Prevalence of  
529 vascular complications among patients with glucokinase mutations and prolonged, mild  
530 hyperglycemia. *JAMA* 311(3): 279-286. 10.1001/jama.2013.283980
- 531 [7] Chakera AJ, Steele AM, Gloyn AL, et al. (2015) Recognition and Management of Individuals  
532 With Hyperglycemia Because of a Heterozygous Glucokinase Mutation. *Diabetes Care* 38(7):  
533 1383-1392. 10.2337/dc14-2769
- 534 [8] Lotta LA, Gulati P, Day FR, et al. (2017) Integrative genomic analysis implicates limited  
535 peripheral adipose storage capacity in the pathogenesis of human insulin resistance. *Nat Genet*  
536 49(1): 17-26. 10.1038/ng.3714
- 537 [9] Oliveri A, Rebernick RJ, Kuppa A, et al. (2024) Comprehensive genetic study of the insulin  
538 resistance marker TG:HDL-C in the UK Biobank. *Nat Genet* 56(2): 212-221. 10.1038/s41588-023-  
539 01625-2
- 540 [10] Suzuki K, Hatzikotoulas K, Southam L, et al. (2024) Genetic drivers of heterogeneity in type 2  
541 diabetes pathophysiology. *Nature* 627(8003): 347-357. 10.1038/s41586-024-07019-6
- 542 [11] Khera AV, Chaffin M, Aragam KG, et al. (2018) Genome-wide polygenic scores for common  
543 diseases identify individuals with risk equivalent to monogenic mutations. *Nat Genet* 50(9):  
544 1219-1224. 10.1038/s41588-018-0183-z
- 545 [12] Schroeder P, Mandla R, Huerta-Chagoya A, et al. (2023) Rare variant association analysis in  
546 51,256 type 2 diabetes cases and 370,487 controls informs the spectrum of pathogenicity of  
547 monogenic diabetes genes. medRxiv. 10.1101/2023.09.28.23296244
- 548 [13] Kingdom R, Beaumont RN, Wood AR, Weedon MN, Wright CF (2024) Genetic modifiers of

- 549 rare variants in monogenic developmental disorder loci. *Nat Genet* 56(5): 861-868.  
550 10.1038/s41588-024-01710-0
- 551 [14] Fahed AC, Wang M, Homburger JR, et al. (2020) Polygenic background modifies penetrance  
552 of monogenic variants for tier 1 genomic conditions. *Nat Commun* 11(1): 3635. 10.1038/s41467-  
553 020-17374-3
- 554 [15] McCarthy MI (2017) Painting a new picture of personalised medicine for diabetes.  
555 *Diabetologia* 60(5): 793-799. 10.1007/s00125-017-4210-x
- 556 [16] Iwani NA, Jalaludin MY, Zin RM, et al. (2017) Triglyceride to HDL-C Ratio is Associated with  
557 Insulin Resistance in Overweight and Obese Children. *Sci Rep* 7: 40055. 10.1038/srep40055
- 558 [17] McLaughlin T, Abbasi F, Cheal K, Chu J, Lamendola C, Reaven G (2003) Use of metabolic  
559 markers to identify overweight individuals who are insulin resistant. *Ann Intern Med* 139(10):  
560 802-809. 10.7326/0003-4819-139-10-200311180-00007
- 561 [18] Pantoja-Torres B, Toro-Huamanchumo CJ, Urrunaga-Pastor D, et al. (2019) High  
562 triglycerides to HDL-cholesterol ratio is associated with insulin resistance in normal-weight  
563 healthy adults. *Diabetes Metab Syndr* 13(1): 382-388. 10.1016/j.dsx.2018.10.006
- 564 [19] Chiang JK, Lai NS, Chang JK, Koo M (2011) Predicting insulin resistance using the  
565 triglyceride-to-high-density lipoprotein cholesterol ratio in Taiwanese adults. *Cardiovasc*  
566 *Diabetol* 10: 93. 10.1186/1475-2840-10-93
- 567 [20] Das S, Forer L, Schonherr S, et al. (2016) Next-generation genotype imputation service and  
568 methods. *Nat Genet* 48(10): 1284-1287. 10.1038/ng.3656
- 569 [21] Purcell S, Neale B, Todd-Brown K, et al. (2007) PLINK: a tool set for whole-genome  
570 association and population-based linkage analyses. *Am J Hum Genet* 81(3): 559-575.  
571 10.1086/519795
- 572 [22] Qiao J, Zhang Z, Ji S, et al. (2022) A distinct role of STING in regulating glucose homeostasis  
573 through insulin sensitivity and insulin secretion. *Proc Natl Acad Sci U S A* 119(7).  
574 10.1073/pnas.2101848119
- 575 [23] Zhu D, Li X, Ma J, et al. (2022) Dorzagliatin in drug-naive patients with type 2 diabetes: a  
576 randomized, double-blind, placebo-controlled phase 3 trial. *Nat Med* 28(5): 965-973.  
577 10.1038/s41591-022-01802-6
- 578 [24] Syed YY (2022) Dorzagliatin: First Approval. *Drugs* 82(18): 1745-1750. 10.1007/s40265-022-  
579 01813-0
- 580 [25] Haddad D, Dsouza VS, Al-Mulla F, Al Madhoun A (2024) New-Generation Glucokinase  
581 Activators: Potential Game-Changers in Type 2 Diabetes Treatment. *Int J Mol Sci* 25(1).  
582 10.3390/ijms25010571
- 583 [26] Chow E, Wang K, Lim CKP, et al. (2023) Dorzagliatin, a Dual-Acting Glucokinase Activator,

584 Increases Insulin Secretion and Glucose Sensitivity in Glucokinase Maturity-Onset Diabetes of the  
585 Young and Recent-Onset Type 2 Diabetes. *Diabetes* 72(2): 299-308. 10.2337/db22-0708

586 [27] Richards S, Aziz N, Bale S, et al. (2015) Standards and guidelines for the interpretation of  
587 sequence variants: a joint consensus recommendation of the American College of Medical  
588 Genetics and Genomics and the Association for Molecular Pathology. *Genet Med* 17(5): 405-424.  
589 10.1038/gim.2015.30

590 [28] Khera AV, Chaffin M, Wade KH, et al. (2019) Polygenic Prediction of Weight and Obesity  
591 Trajectories from Birth to Adulthood. *Cell* 177(3): 587-596 e589. 10.1016/j.cell.2019.03.028

592 [29] Johansson S, Irgens H, Chudasama KK, et al. (2012) Exome sequencing and genetic testing  
593 for MODY. *PLoS One* 7(5): e38050. 10.1371/journal.pone.0038050

594 [30] Udler MS, McCarthy MI, Florez JC, Mahajan A (2019) Genetic Risk Scores for Diabetes  
595 Diagnosis and Precision Medicine. *Endocr Rev* 40(6): 1500-1520. 10.1210/er.2019-00088

596 [31] Bonnefond A, Semple RK (2022) Achievements, prospects and challenges in precision care  
597 for monogenic insulin-deficient and insulin-resistant diabetes. *Diabetologia* 65(11): 1782-1795.  
598 10.1007/s00125-022-05720-7

599 [32] Pearson ER, Velho G, Clark P, et al. (2001) beta-cell genes and diabetes: quantitative and  
600 qualitative differences in the pathophysiology of hepatic nuclear factor-1alpha and glucokinase  
601 mutations. *Diabetes* 50 Suppl 1: S101-107. 10.2337/diabetes.50.2007.s101

602 [33] McCarthy MI (2010) Genomics, type 2 diabetes, and obesity. *N Engl J Med* 363(24): 2339-  
603 2350. 10.1056/NEJMra0906948

604 [34] Le Collen L, Froguel P, Bonnefond A (2024) Towards the recognition of oligogenic forms of  
605 type 2 diabetes. *Trends Endocrinol Metab*. 10.1016/j.tem.2024.06.006

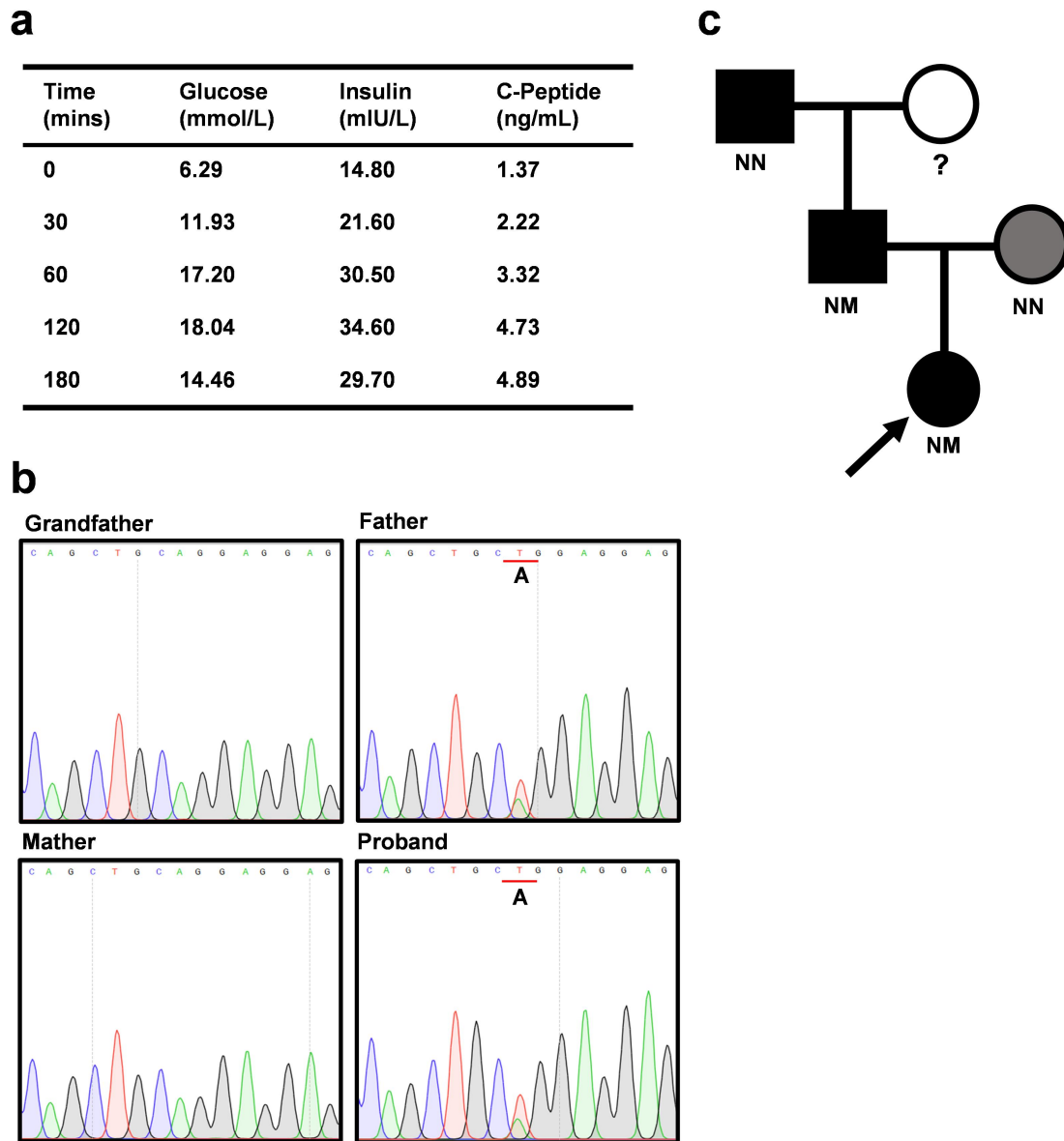
606 [35] Inshaw JRJ, Cutler AJ, Crouch DJM, Wicker LS, Todd JA (2020) Genetic Variants Predisposing  
607 Most Strongly to Type 1 Diabetes Diagnosed Under Age 7 Years Lie Near Candidate Genes That  
608 Function in the Immune System and in Pancreatic beta-Cells. *Diabetes Care* 43(1): 169-177.  
609 10.2337/dc19-0803

610

611

612

613

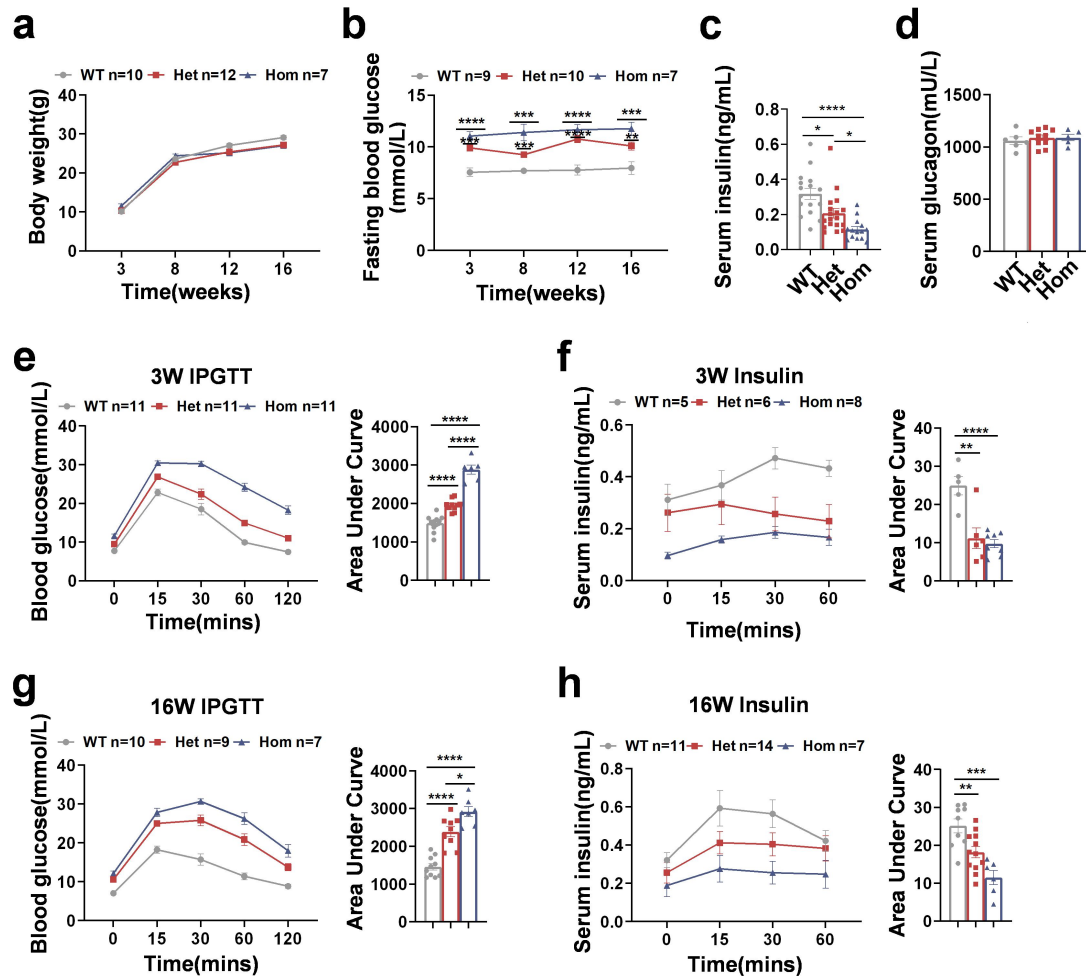


1

2 **Figure 1. Proband with impaired insulin secretion and diabetes carries a GCK missense**  
 3 **mutation (c.77A>T, p.Q26L) that was inherited from her father. (a) The results of blood**  
 4 **glucose, insulin, and C-Peptide of the proband during OGTT performed at the onset of diabetes. (b)**  
 5 **A missense mutation in GCK gene (c.77A>T, p.Q26L) was identified in the proband and her**  
 6 **father by WES confirmed by Sanger sequencing. (c) Pedigree analyses showed that GCK-Q26L**  
 7 **was inherited from proband's father. Squares represent males and circles represent females. Filled**  
 8 **black symbols indicated members affected with diabetes, gray symbol represented the member**  
 9 **with the pre-diabetes. The proband was indicated with a black arrow. Where tested, the genotypes**  
 10 **of family members were given (N, normal allele; M, mutant allele; NN, normal genotype; NM,**

11 heterozygous genotype).

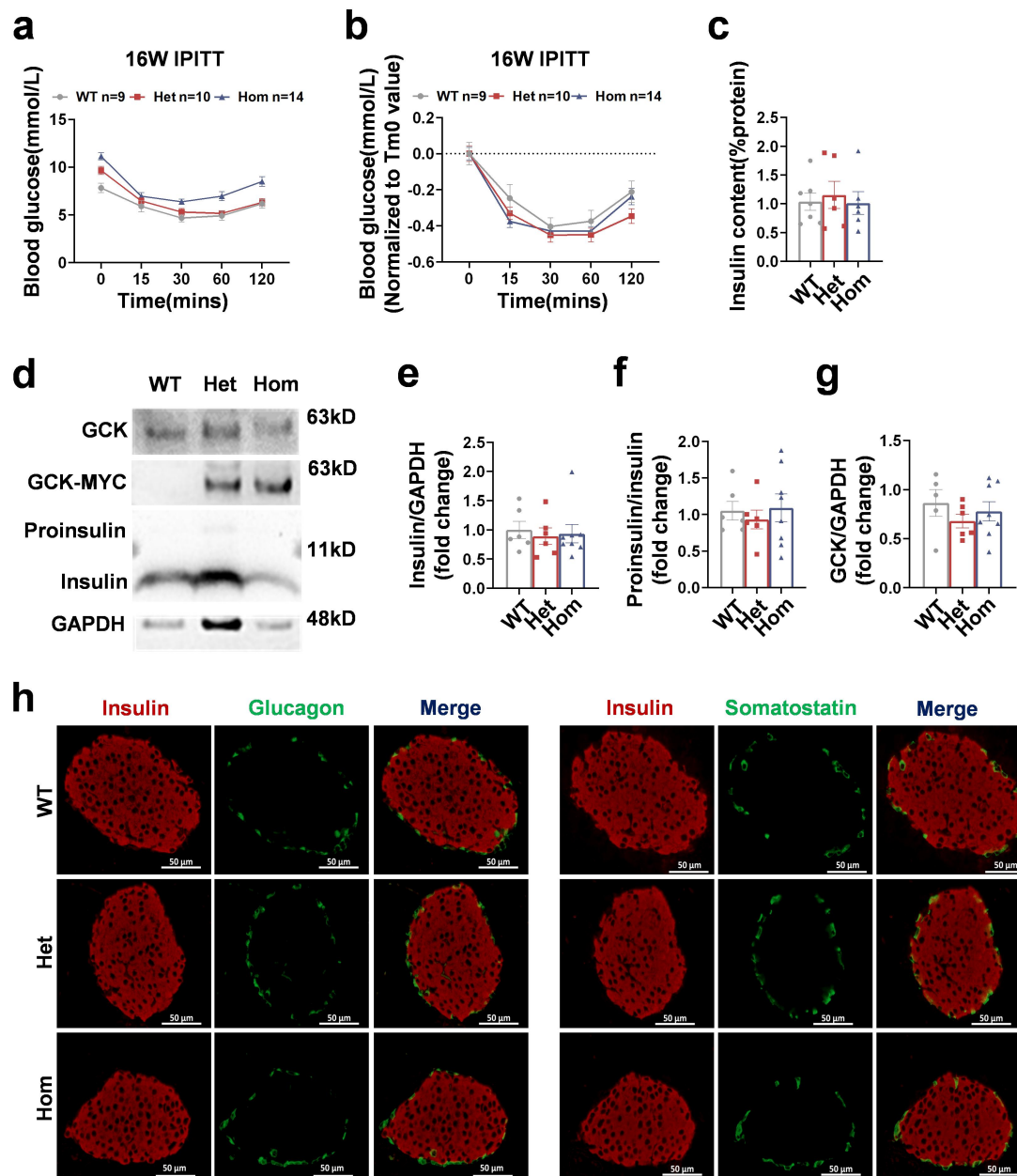




12

13 **Figure 2. GCK-Q26L causes glucose intolerance in a dose-dependent manner.** (a, b) Body  
 14 weight (a) and fasting blood glucose (b) of male mice were measured at 3, 8, 12, 16 weeks of age.  
 15 WT vs Het, WT vs Hom, \*\* P < 0.01, \*\*\* P < 0.001, \*\*\*\* P < 0.0001. (c) Fasting serum insulin in  
 16 three-group 16-week-old male mice were measured by ELISA. (d) Fasting serum glucagon in  
 17 three-group 16-week-old male mice were measured by ELISA. (e) IPGTT in 3-week-old male  
 18 mice (2 g/kg i.p.) and the area under curve (AUC) of blood glucose during IPGTT. (f) Serum  
 19 insulin levels in 3-week-old male mice during IPGTT were measured by ELISA, with calculated  
 20 AUCs. (g) IPGTT in 16-week-old male mice (2 g/kg i.p) and the AUC of blood glucose. (h)  
 21 Serum insulin levels in 16-week-old male mice during IPGTT were measured by ELISA, with  
 22 calculated AUCs. Each data point represents an individual mouse. Values are shown as mean ±  
 23 SEM. WT vs Het, WT vs Hom, Het vs Hom, \*P < 0.05, \*\*\*\* P < 0.0001.

24



25

26 **Figure 3. GCK-Q26L did not affect insulin sensitivity, insulin content, and islet cell**  
 27 **composition. (a, b)** IPITT were performed in 16-week-old male mice (0.7 U/kg i.p), **(b)** was **(a)**  
 28 normalized to the baseline of blood glucose. **(c)** Islet insulin content of 16-week-old male mice  
 29 was measured by ELISA. **(d)** Islets isolated from 10-week-old male mice were directly lysed.  
 30 Western blots were performed to detect endogenous GCK, MYC-tagged GCK (GCK-MYC),  
 31 proinsulin and insulin as indicated. GAPDH was used as a loading control. Quantification of  
 32 insulin **(e)**, the ratio of proinsulin to insulin **(f)**, and GCK **(g)**. **(h)** Representative  
 33 immunofluorescence images of anti-insulin (red), anti-glucagon (green) and

34 anti-somatostatin(green) antibodies in pancreatic sections from 12-week-old male mice. Scale bar  
35 = 50  $\mu\text{m}$  (n = 3 mice/group). Each data point represents an individual mouse. Values were shown  
36 as mean  $\pm$  SEM.

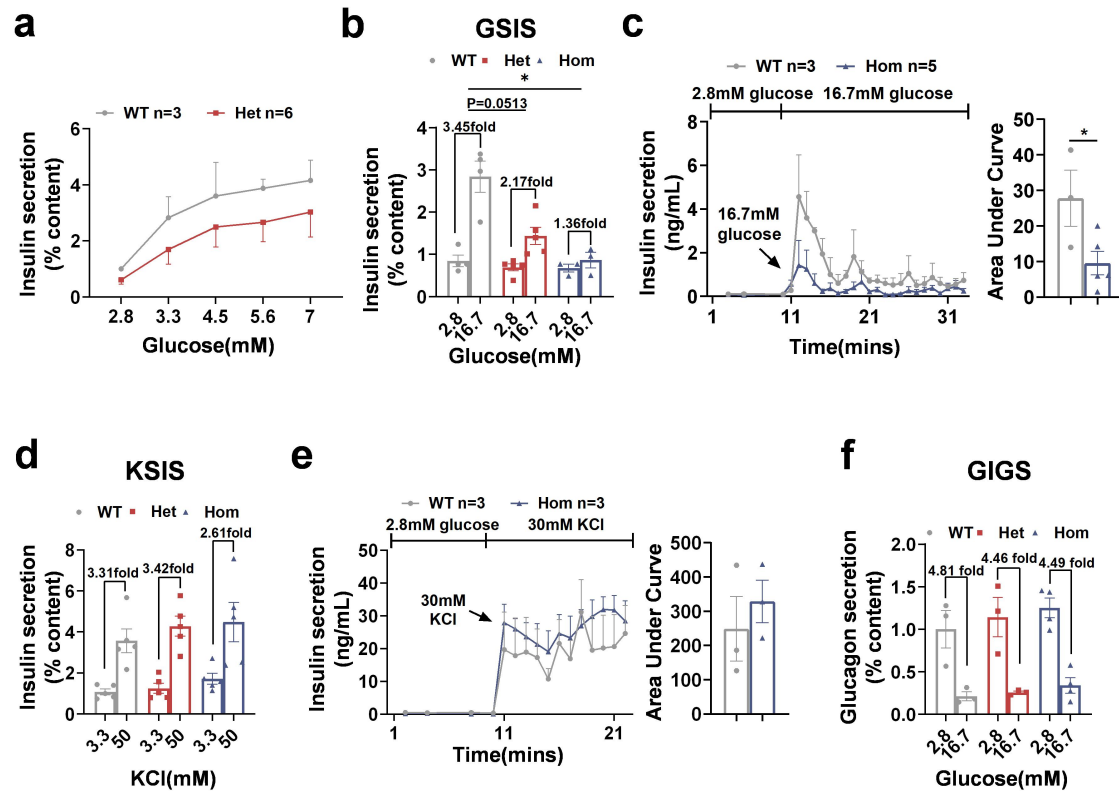


**Figure 4. GCK-Q26L impaired glucose-stimulated insulin secretion without affecting potassium-stimulated insulin secretion and glucose-inhibited glucagon secretion.** (a) Dose-dependent effects of glucose on insulin secretion of 16-week-old male WT and Het mice. Isolated islets successively incubated in 2.8, 3.3, 4.5, 5.6 and 7 mmol/L glucose. (b) Islets isolated from 10-week-old male WT, Het and Hom mice were incubated with 2.8 mmol/L for 1 hour followed by stimulated with either low (2.8 mmol/L) or high (16.7 mmol/L) glucose for 2 hours. Insulin secretion response to low and high glucose were measured. (c, e) Dynamic insulin secretion of 10-week-old male WT and Hom mice islets cultured in the perfusion chamber with continuous buffer renewal (2.8 mmol/L glucose, 16.7 mmol/L glucose, 2.8 mmol/L glucose, 30 mmol/L potassium), with calculated AUCs. (d) Islets isolated from 10-week-old male WT, Het and Hom mice were incubated with 2.8 mmol/L glucose for 1 hour followed by stimulated with either low (3.3 mmol/L) or high (50 mmol/L) potassium for 2 hours. Insulin secretion response to low and high potassium were measured. (f) Glucagon secretion measured in isolated islets from 10-week-old male WT, Het and Hom mice when incubated in 2.8 and 16.7 mmol/L glucose. Each data point represents an individual mouse. Values are shown as mean  $\pm$  SEM. \* P < 0.05.

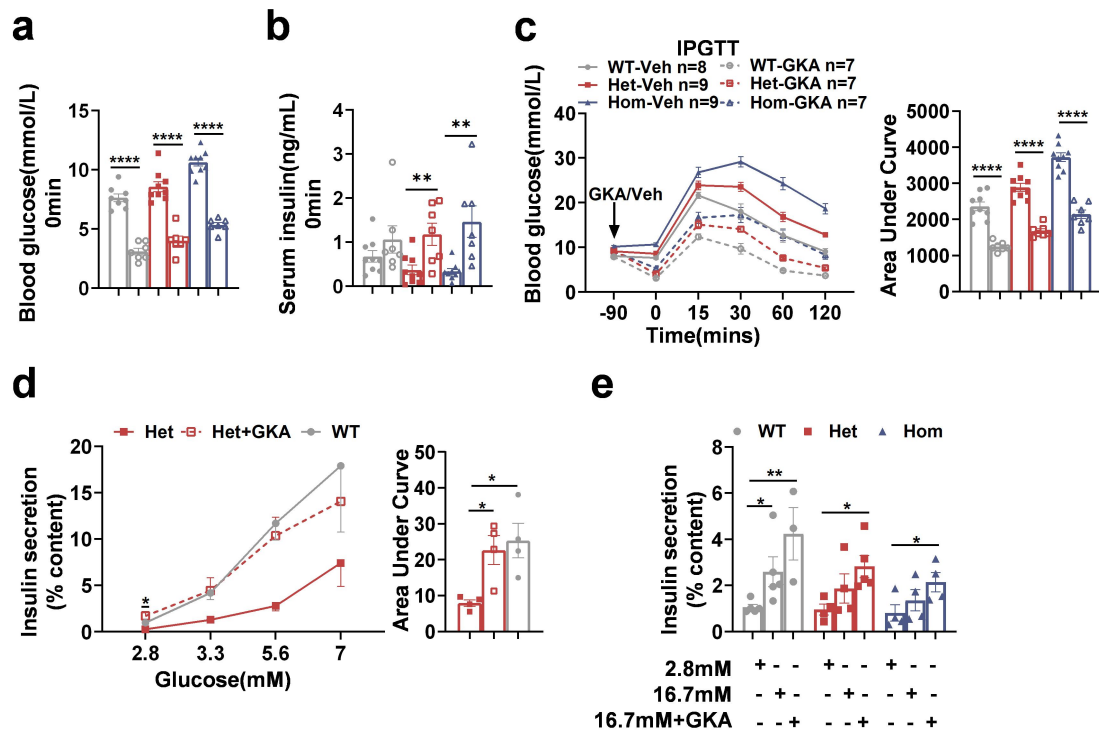


**Figure 5. Dorzagliatin (GKA) restores the glucose threshold for insulin secretion and ameliorates glucose tolerance in GCK-Q26L mice.** (a-c) We performed IPGTT on 10-week-old male mice (2 g/kg i.p), and vehicle (0.9% Nacl) or GKA (30 mg/kg) was administered orally to mice 90 minutes before glucose challenge. Blood glucose (a) and serum insulin level (b) before glucose challenge. (c) Blood glucose and AUC of IPGTT. (d) Dose-dependent effects of glucose on insulin secretion of 10-week-old male WT and Het mice with or without 30  $\mu$ M GKA, and the AUC of Insulin secretion. Het vs Het-GKA, \* $P < 0.05$ . (e) Insulin secretion measured in isolated islets from 10-week-old male WT, Het and Hom mice when incubated in 2.8, 16.7 mmol/L glucose and 16.7 mmol/L glucose containing 30  $\mu$ M GKA. Each data point represents an individual mouse. Values are shown as mean  $\pm$  SEM. \*  $P < 0.05$ , \*\*  $P < 0.01$ , \*\*\*\*  $P < 0.0001$ .

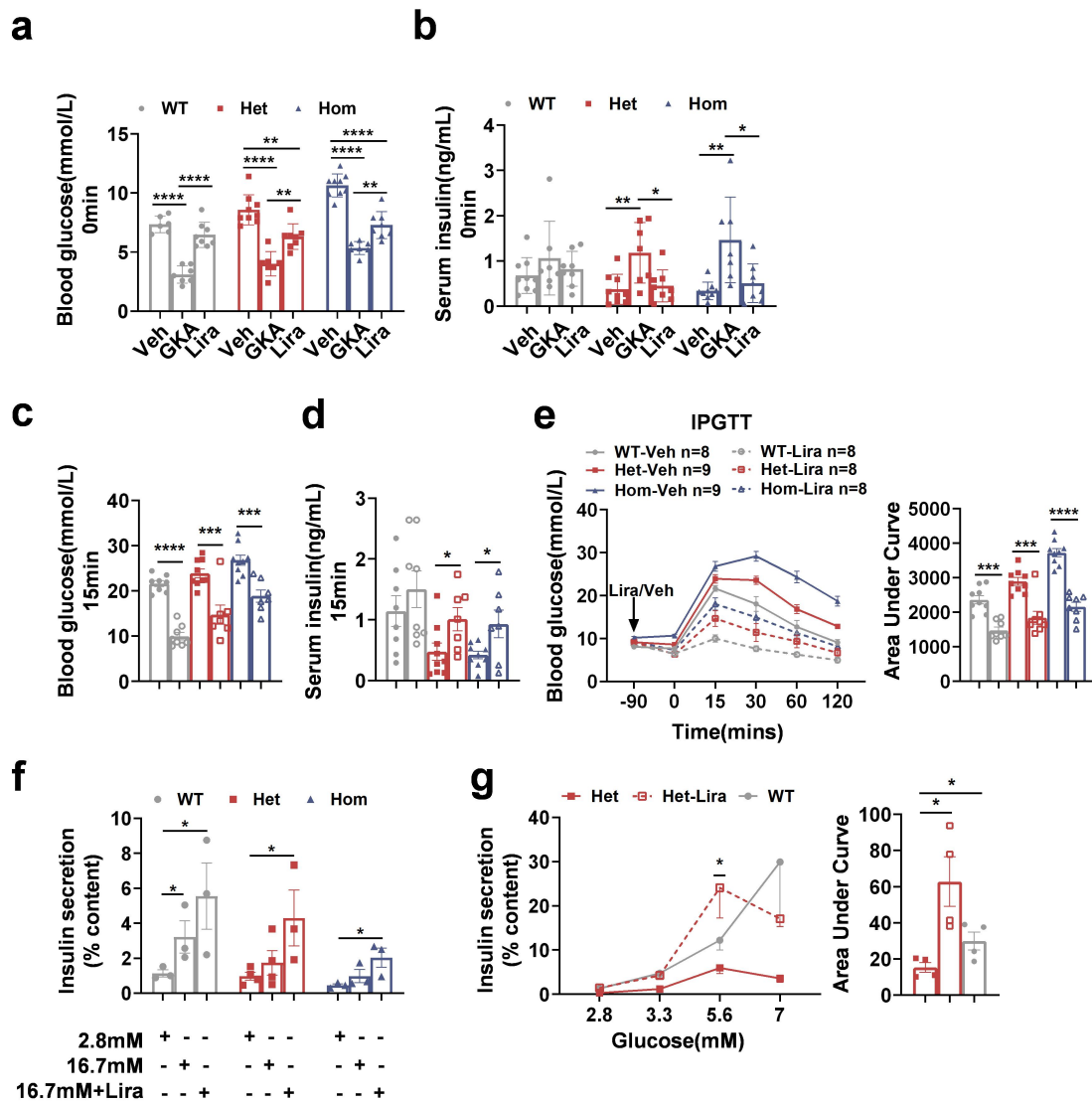


**Figure 6. Liraglutide amplifies insulin secretion response to glucose and ameliorates glucose tolerance in GCK-Q26L mice.** (a, b) For liraglutide, we conducted experiments similar to those shown in Figure 5 with dorzagliatin, assessing blood glucose (a) and serum insulin levels (b) in mice that had been treated with dorzagliatin and liraglutide prior to glucose challenge. (c-e) show the results of IPGTT with Liraglutide. Blood glucose (c) and serum insulin level (d) 15 minutes after glucose challenge. (e) IPGTT and the AUC of blood glucose. (f) Insulin secretion measured in isolated islets from 10-week-old male WT, Het and Hom mice when incubated in 2.8, 16.7 mmol/L glucose and 16.7 mmol/L glucose containing 100 nM Lira. (g) Dose-dependent effects of glucose on insulin secretion and the AUC of 10-week-old male WT and Het mice with or without 100 nM Lira, Het vs Het-Lira, \* P < 0.05. Each data point represents an individual mouse. Values are shown as mean ± SEM. \* P < 0.05 \*\*\* P < 0.001, \*\*\*\* P < 0.0001.

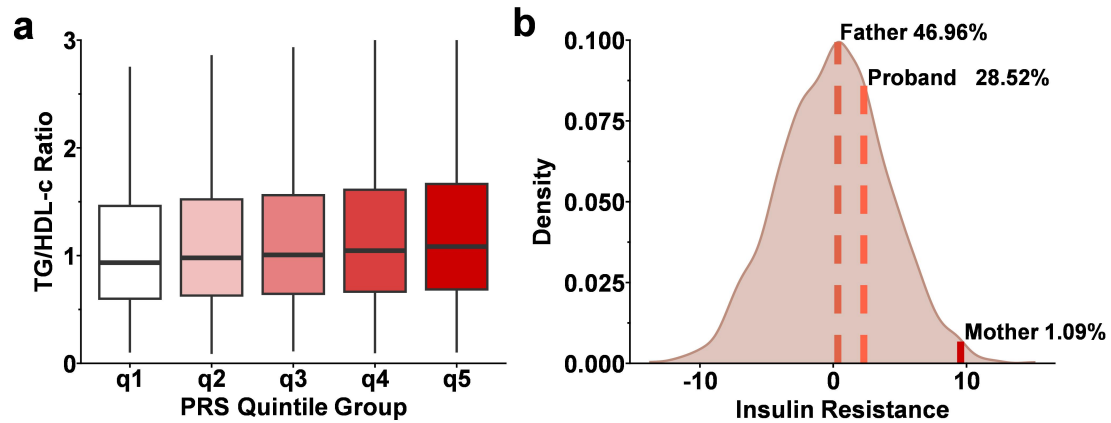


**Figure 7. Quality control and PRS score for study samples.** (a) The distribution of the ratio of triglycerides to HDL cholesterol as a function of quintiles of an insulin resistance (IR) polygenic risk score (PRS) was evaluated in 424,664 UK Biobank samples. The horizontal line in the box indicates the median value, and the top and bottom of the box indicate the upper and lower quartiles, respectively. (b) The results of insulin resistance polygenic risk score analysis on case family. The curve denotes the probability density function of the IR PRS scores from the 1000 Genomes Project East Asian samples. Vertical dashed lines indicate the PRS for each family member: the father's position at the top 46.96<sup>th</sup> percentile, the proband at the top 28.52<sup>th</sup> percentile, and the mother at the top 1.09<sup>th</sup> percentile.

**Table 1. Clinical features of the family of the proband carrying GCK(Q26L) mutation**

	<b>Proband</b>	<b>Father</b>	<b>Mother</b>
<b>Age at diagnosis</b>	Teens	Thirties	/
<b>Gender</b>	Female	Male	Female
<b>BMI at present (kg/m<sup>2</sup>)</b>	26.76	25.54	29.78
<b>Clinical symptoms at onset</b>	Polydipsia, polyuria, polyphagia, weight loss and ketosis	found elevated FBG in a physical examination	/
<b>FBG at diagnosis (mmol/L)</b>	6-7	5-7	/
<b>FBG at present (mmol/L)</b>	7.5-13.2	6.5	6.4
<b>HbA1c at diagnosis (mmol/mol)</b>	113.12 (12.5%)	/	/
<b>HbA1c at present (mmol/mol)</b>	132.79 (14.3%)	60.66 (7.7%)	44.26 (6.2%)
<b>Total cholesterol (mmol/L)</b>	5.85	5.44	4.19
<b>Triglycerides (mmol/L)</b>	10.39	0.80	1.11
<b>HDL-cholesterol (mmol/L)</b>	0.74	1.03	0.78
<b>LDL-cholesterol (mmol/L)</b>	3.88	3.90	3.24
<b>Islet autoantibodies</b>	Negative	/	/
<b>Treatment at diagnosis</b>	Metformin 0.5g TID	Metformin 0.5g BID	/



<b>Treatment at present</b>	Insulin glargine: 18U QN	Vildagliptin 50mg BID	
	Metformin 0.5g TID	Metformin 0.5g BID	/
	Insulin aspart: 8-6-6U		
	Insulin glargine: 12U QN		
<b>Complications and comorbidities</b>	No	Diabetic retinopathy (non-proliferative stage)	/

---

Note: BMI, body mass index; FBG, fasting blood glucose; HDL, high density lipoprotein; LDL, low density lipoprotein; OGTT, oral glucose tolerance test; OHA, oral hypoglycemic agent; Islet autoantibodies, GADA(glutamate decarboxylase antibody)、ICA(islet cell antibody)、 IA-2A(protein tyrosine phosphatase-like protein antigen)、 ZnT8A(Zinc transporter 8 antibody); TID, ter in die; BID, bis in die; QN, quāque nocte; “/”, none or not provided.